Journal of Radiation Research, Vol. 65, No. 3, 2024, pp. 263–271
https://doi.org/10.1093/jrr/rrae005
Advance Access Publication: 8 March 2024

Inhibition of intracellular ATP synthesis impairs the recruitment of homologous recombination factors after ionizing radiation

Ryota Hayashi[1], Hikaru Okumura[1], Mayu Isono[1], Motohiro Yamauchi[2], Daiki Unami[1], Rahmartani Tania Lusi[3], Masamichi Yamamoto[4], Yu Kato[1], Yuki Uchihara[1] and Atsushi Shibata[1,*]

[1]Division of Molecular Oncological Pharmacy, Faculty of Pharmacy, Keio University, 1-5-30 Shibakoen, Minato-ku, Tokyo 105-8512, Japan
[2]Hospital Campus Laboratory, Radioisotope Center, Central Institute of Radioisotope Science and Safety Management, Kyushu University, 3-1-1 Maidashi, Higashi-ku, Fukuoka 812-8582, Japan
[3]Department of Radiation Oncology, Faculty of Medicine Universitas Indonesia – Dr. Cipto Mangunkusumo National General Hospital, Jl. Diponegoro No.71, Jakarta Pusat, DKI Jakarta 10430, Indonesia
[4]Department of Research Promotion and Management, National Cerebral and Cardiovascular Center, 6-1 Kishibe-Shimmachi, Suita, Osaka 564-8565, Japan
*Corresponding author. Division of Molecular Oncological Pharmacy, Faculty of Pharmacy, Keio University, 1-5-30 Shibakoen, Minato-ku, Tokyo 105-8512, Japan. Tel: +81-3-5400-2670; Email: shibata.at@keio.jp
(Received 19 October 2023; revised 16 January 2024; editorial decision 19 January 2024)

ABSTRACT

Ionizing radiation (IR)-induced double-strand breaks (DSBs) are primarily repaired by non-homologous end joining or homologous recombination (HR) in human cells. DSB repair requires adenosine-5′-triphosphate (ATP) for protein kinase activities in the multiple steps of DSB repair, such as DNA ligation, chromatin remodeling, and DNA damage signaling via protein kinase and ATPase activities. To investigate whether low ATP culture conditions affect the recruitment of repair proteins at DSB sites, IR-induced foci were examined in the presence of ATP synthesis inhibitors. We found that p53 binding protein 1 foci formation was modestly reduced under low ATP conditions after IR, although phosphorylated histone H2AX and mediator of DNA damage checkpoint 1 foci formation were not impaired. Next, we examined the foci formation of breast cancer susceptibility gene I (BRCA1), replication protein A (RPA) and radiation 51 (RAD51), which are HR factors, in G2 phase cells following IR. Interestingly, BRCA1 and RPA foci in the G2 phase were significantly reduced under low ATP conditions compared to that under normal culture conditions. Notably, RAD51 foci were drastically impaired under low ATP conditions. These results suggest that HR does not effectively progress under low ATP conditions; in particular, ATP shortages impair downstream steps in HR, such as RAD51 loading. Taken together, these results suggest that the maintenance of cellular ATP levels is critical for DNA damage response and HR progression after IR.

Keywords: DSB repair; ATP shortage; ionizing radiation; foci formation; homologous recombination

INTRODUCTION

Ionizing radiation (IR) causes deoxyribonucleic acid (DNA) double-strand breaks (DSBs), which are toxic and mutagenic lesions leading to genomic instability. Failure of DSB repair causes chromosomal aberrations, such as deletions, translocations and dicentric chromosomes, which may lead to the development of cancer, aging or neurodegeneration [1, 2]. In addition, DSBs are induced by radiotherapy, and several chemotherapeutic agents (e.g. cisplatin and alkylating agents) promote cancer cell death [3, 4].

The introduction of DSBs after IR promotes the recruitment of DNA repair proteins and signal transduction. Immediately after the induction of DSBs, activated ataxia telangiectasia-mutated (ATM) protein at these breaks phosphorylates a thousand of downstream proteins and promotes signal transduction; for example, for cell-cycle checkpoint arrest or for apoptosis. ATM also phosphorylates histone H2AX (the phosphorylated form of H2AX is called γH2AX) and γH2AX recruits the mediator of DNA damage checkpoint 1 (MDC1) [5, 6], which also recruits two ubiquitin ligases, ring finger

protein 8 (RNF8) and RNF168 [7–9], followed by the recruitment of p53 binding protein 1 (53BP1) [10]. In human cells, DSBs are primarily repaired by either non-homologous end joining (NHEJ) or homologous recombination (HR) [1]. The selection of the DSB repair pathway is regulated by the cell-cycle phase; that is, NHEJ contributes to DSB repair throughout the cell-cycle phases except for the M phase, whereas HR functions only in the S and G2 phases [11, 12]. In NHEJ, DNA-PKcs and Ku70/80 heterodimer complex initiate the NHEJ process, and the DNA ligase IV ligates break ends under support with XRCC4 and XLF. In HR, DSB end resection, which generates a 3′ single-strand DNA (ssDNA) overhang, is an essential step of HR initiation. DSB resection is upregulated by the CDK activity during the S/G2 phase. MRE11 and CtIP initiate DSB end resection, followed by resection extension using EXO1/DNA2/BLM [1, 13–16]. Breast cancer susceptibility gene I (BRCA1) promotes this process through multiple functions [17]. Following resection, the generated ssDNA was coated with replication protein A (RPA). Subsequently, BRCA1 and BRCA2 facilitate the switch from RPA to radiation 51 (RAD51) in ssDNA. RAD51-coated ssDNA promotes strand invasion and recombination with the sister chromatid template. In both DSB repair and signal transduction, multiple protein kinases phosphorylates downstream factors; that is, cells utilize adenosine-5′-triphosphate (ATP) during DSB repair process and ATP is also used for DNA ligation, DNA nuclease, DNA helicase and chromatin remodeling. However, whether cellular ATP shortages affect DSB repair after IR is not fully understood. In addition, the investigation of DSB repair under low ATP conditions is important for understanding the genome stability in human diseases because, for example, cerebral ischemia and myocardial infarction cause hypoxia, which results in a decrease in the ATP concentration [18].

In this study, we aimed to investigate the impact of reduced ATP levels on the formation of DSB repair foci, such as γH2AX, MDC1, 53BP1, BRCA1, RPA and RAD51, which represent DNA damage signaling and HR repair capability following IR. We used cell culture conditions showing ∼80% reduction in the intracellular ATP levels in the presence of two ATP synthesis inhibitors, namely oligomycin A (OM) and 2-deoxy-D-glucose (2DG). Our analysis revealed that γH2AX and MDC1 foci formation remained unaffected under low ATP conditions after IR. However, 53BP1 foci formation was modestly reduced. Subsequently, we found a reduction in the formation of BRCA1 and RPA foci in G2 phase cells under conditions of low ATP levels compared with standard culture conditions. Remarkably, the formation of RAD51 foci in G2 phase cells was significantly impaired in the presence of low ATP levels. These findings suggest that the HR efficacy is limited at low ATP levels. Collectively, these results suggest the critical role of maintaining cellular ATP levels for an efficient DNA damage response and proper progression of HR following IR.

MATERIALS AND METHODS

Cell culture, irradiation and drug treatment

The human retinal pigment epithelial (RPE)-hTERT (Clontech) cell line was cultured in Dulbecco's Modified Eagle's Medium: nutrient mixture F-12 (Fujifilm Wako Pure Chemical Industries, Ltd, Osaka, Japan) supplemented with 10% fetal bovine serum (SERANA, Brandenburg, Germany), 1× penicillin–streptomycin-L-glutamine solution (Fujifilm Wako Pure Chemical Industries, Ltd) and sodium bicarbonate (Fujifilm Wako Pure Chemical Industries, Ltd). In this study, RPE-hTERT is described as RPE unless stated otherwise. The RPE cells were cultured at 37°C with 5% CO_2. X-ray irradiation was performed using MX-160Labo (160 kVp, 1.07 Gy/min, 3.00 mA, MediXtec, Chiba, Japan). An ATM inhibitor (ATMi) (KU55933) (#587871-26-9; Merck Life Science, Darmstadt, Germany) was added 30 min prior to the IR. For the ATP synthesis inhibitors, 10 μM OM (#S1478; Selleck Chemicals, Houston, TX, USA) and 20 mM 2DG (#040–06481; Fujifilm Wako Pure Chemical Industries, Ltd) were added 2 h before IR. Next, 3 μM aphidicolin (APH) (#011-09811; Fujifilm Wako Pure Chemical Industries, Ltd) was added immediately after IR to block the S to G2 phase progression.

Immunofluorescence staining and microscopy

The RPE cells were seeded on Cover Glass No. 1 (Matsunami, Osaka, Japan) 48 h before IR to obtain cells in the exponential growth phase. Cells in the G2 phase were identified using centromere protein-F (CENPF) staining. To identify the cells in S phase, 5-ethynyl-2′-deoxyuridine (EdU) (#052-08843; Fujifilm Wako Pure Chemical Industries, Ltd) staining was performed. EdU (10 μM) was added 2.5 h before IR. At indicated time points, cells were fixed for 10 min in 3% paraformaldehyde–2% sucrose and were permeabilized for 3 min with 0.2% TritonX-100 in phosphate-buffered saline (PBS). Cells were washed twice with PBS and were incubated at 37°C for 30 min with the primary antibody in 2% bovine serum albumin (BSA) in PBS. Cells were then washed twice with PBS and were incubated at 37°C for 30 min with secondary antibodies conjugated with Alexa Fluor 488 or 594 in 2% BSA in PBS. Subsequently, cells were washed twice with PBS and were incubated at 37°C for 30 min with EdU detection solution (Alexa Fluor 647 azide [1:500, #A10277; Invitrogen, Carlsbad, CA, USA] in 100 mM Tris–HCl [pH 7.5] [#318-90225; Nippon Gene Co., Ltd, Tokyo, Japan], 4 mM $CuSO_4$ [#000-18522; Kishida Chemical Co., Ltd, Osaka, Japan] and 100 mM Ascorbic Acid [#000-05732; Kishida Chemical Co., Ltd]). After an additional wash with PBS, the cover glasses were mounted on slide glasses (Matsunami) using ProLong Gold Antifade Reagent with 4′, 6-diamidino-2-phenylindole (DAPI) (#8961; Cell Signaling Technology, Danvers, MA, USA). To analyze chromatin-bound BRCA1, RPA and RAD51, cells were treated with 0.2% TritonX-100 in PBS for 1 min before fixation. The following primary antibodies were used: anti-γH2AX (1:800, #05-636; Merck Millipore, Burlington, MA, USA), anti-MDC1 (1:400, #A300-053A; Bethyl Laboratories, Inc., Montgomery, TX, USA), anti-53BP1 (1:2000, #A300-272A; Bethyl Laboratories), anti-BRCA1 (1:200, #sc-6954; Santa Cruz Biotechnology, Inc., Dallas, TX, USA), anti-RPA (1:800, #LC-C38952; LifeSpan BioSciences, Shirley, MA, USA), anti-RAD51 (1:100, #sc-8349; Santa Cruz Biotechnology, Inc.), mouse anti-CENPF (Mitosin) (1:250, #610768; BD Transduction Laboratories, Franklin Lakes, NJ, USA) and rabbit anti-CENPF (1:250, #58982; Cell Signaling Technology). The following secondary antibodies were used: anti-rabbit IgG (H + L), $F(ab')_2$ fragment (Alexa Fluor 594 conjugate) (1:500, #8889; Cell Signaling Technology), anti-mouse IgG (H + L), $F(ab')_2$ fragment (Alexa Fluor 488 conjugate) (1:500, #4408; Cell Signaling Technology) and anti-rat IgG (H + L), (Alexa Fluor 488 Conjugate) (1:500, #4416; Cell Signaling Technology). Focus scoring was performed blindly by scoring 30 cells per sample.

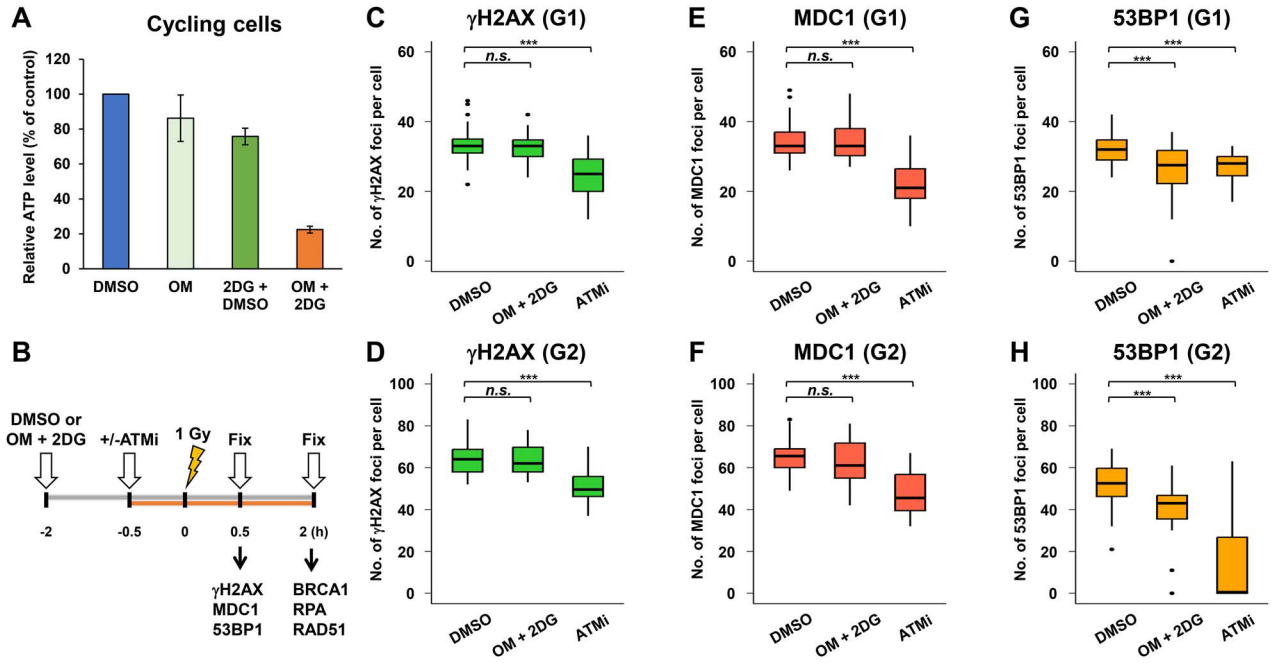

Fig. 1. Analysis of DNA repair foci formation under low ATP conditions in G1 and G2 phase cells after IR. (A) Treatment with OM + 2DG reduced ATP to 20% in DMSO-treated control cells. DMSO, 10 μM OM, 20 mM 2DG or 10 μM OM + 20 mM 2DG was added to RPE cells 2 h prior to the measurement of intracellular ATP levels using the ATP Assay kit. ATP levels were normalized to those in DMSO-treated control cells. Error bars represent SD from three independent experiments. (B) A representative diagram of experimental scheme. (C–H) 53BP1 foci formation was modestly reduced under low ATP conditions, whereas γH2AX and MDC1 foci formation were not impaired. RPE cells were irradiated with 1 Gy IR. The initial recruitment of DSB repair proteins was analyzed 30 min after IR. To prevent the progression of S phase cells into the G2 phase during analysis, a replicative polymerase inhibitor, 3 μM APH, was added immediately after IR. APH alone did not affect DSB repair in G2 phase cells [21]. DMSO or 10 μM OM + 20 mM 2DG were added 2 h before IR irradiation. ATMi was added 30 min before IR. A box plot was generated based on the results of a single experiment. Similar results were obtained from two independent experiments. Statistical analyses were performed for a single experiment (C–H). $^{***}P < 0.001$, n.s., not significant.

Representative images were taken using an ECLIPSE Ni-U with DS-Qi2 camera and NIS-Elements D (Nikon Corporation, Tokyo, Japan). For the foci intensity analysis, microscopic images were taken using an Applied Precision DeltaVision OMX microscope with a 60× objective lens. *Z* stacks were taken over 2–3-μm areas (sections taken every 0.25 μm), and individual nuclei were imaged. Deconvolution was performed using softWoRx software. In such a case that 53BP1, RPA and RAD51 foci may not be formed at some DSB sites, each foci intensity within γH2AX was measured with Imaris 8.2.1 (Oxford Instruments, Abingdon, UK). Polygon rendering was generated by using Imaris 8.2.1 (Oxford Instruments).

Cellular ATP measurement

RPE cells (2×10^3 cells) were plated in 96-well plates for 24 h. The medium was refreshed, and dimethyl sulfoxide (DMSO) (#13408-64; Nacalai Tesque, Inc., Kyoto, Japan), the concentration of which was equalized between the control- and inhibitor-treated groups, 10 μM OM, 20 mM 2DG or 10 μM OM + 20 mM 2DG was added. After 2 h, the intracellular ATP levels were measured using an ATP assay kit (Dojindo Laboratories, Kumamoto, Japan) according to the manufacturer's protocol.

Immunoblotting

Immunoblotting was performed using whole-cell lysates. Following boiling for 5 min at 95°C, cell lysates were sonicated using Q55 Sonicator (Qsonica, Newtown, CT, USA). The sample was run on 7.5% or 4–20% Mini-PROTEAN TGX precast gels (Bio-Rad Laboratories, Hercules, CA, USA) for 30–35 min at 200 V. Then, the gels were transferred onto a nitrocellulose membrane (Pall Corporation, Port Washington, NY, USA) for 60 min at 100 V. The transferred membrane was blocked using 5% nonfat dry milk (#9999; Cell Signaling Technology) for 30 min and was incubated with a primary antibody overnight at room temperature. The membrane was washed and incubated with a secondary antibody for 60 min at room temperature. Following the washing of the membrane, the chemical luminescence signal was detected using Amersham Imager 600 (Amersham, Little Chalfont, UK) and Amersham ECL Western Blotting Detection Reagent (Amersham). The following primary antibodies were used: anti-H2AX (1:2000, #ab11175; Abcam, Cambridge, UK), anti-MDC1 (1:1000), anti-53BP1 (1:2000), anti-BRCA1 (1:500), anti-RPA (1:1000), anti-RAD51 (1:500), anti-Ku80 (1:2000, #2180; Cell Signaling Technology), anti-ATM (1:1000, #ab81292; Abcam) and anti-ATM phosho-S1981 (1:500, #2873;

Fig. 2. Representative images of IR-induced foci formation under low ATP conditions. (A–F) Representative images of IR-induced γH2AX, MDC1 and 53BP1 foci in G1 or G2 phase RPE cells 30 min after 1 Gy IR, as shown in Fig. 1. DMSO or 10 μM OM + 20 mM 2DG were added 2 h before IR irradiation. ATMi was added 30 min before IR. For G2 phase foci analysis, 3 μM APH was added immediately after IR. Irradiated RPE cells were fixed and stained for (A, B) γH2AX and CENPF (G2 phase marker), (C, D) MDC1 and CENPF and (E, F) 53BP1 and CENPF. DNA was stained with DAPI. Scale bar, 10 μm.

Cell Signaling Technology). The following secondary antibodies were used: anti-rabbit IgG, HRP-linked antibody (1:4000, #7074; Cell Signaling Technology), anti-mouse IgG, HRP-linked antibody (1:4000, #7076; Cell Signal Technology) and anti-rat IgG, HRP-linked antibody (1:4000, #7077; Cell Signaling Technology). The intensity of each band was measured using ImageJ (version 2.14.0).

Quantification and statistical analysis

Foci scoring in the immunofluorescence study was performed blindly, with 30 cells per sample. Box plots were created using ggplot2 in R 4.2.1. Statistical significance was determined using the two-tailed Student's *t*-test or Welch's *t*-test. If the Shapiro–Wilk test failed, the Mann–Whitney U test was used. Bonferroni's correction was applied when multiple comparisons were performed. All data were derived from two or three independent experiments. The significance levels are shown in each panel as follows: $^{***}P < 0.001$, n.s., not significant.

RESULTS

To investigate whether low ATP levels in tissue culture conditions influence the DSB repair capability in normal human cells, foci analysis was performed in RPE cells after IR. To obtain low ATP conditions in tissue cultures, two distinct ATP synthesis inhibitors were used in this study (OM is a mitochondrial ATP synthesis inhibitor and 2DG is a glycolytic inhibitor). To confirm the reduction in ATP levels, intracellular ATP levels were examined following treatment with inhibitors for 2 h. OM and 2DG reduced the ATP levels to ∼85 and 75% of the control, corresponding to a decrease of 15 and 25% in ATP levels, respectively. However, we did not observe substantial changes in DSB repair foci formation at this range of ATP reduction (data not shown). Because single-drug treatment did not sufficiently reduce the cellular ATP levels, we treated the cells with both inhibitors. Importantly, treatment with both OM and 2DG achieved an 80% reduction in ATP levels (Fig. 1A). These results suggest that inhibition of both mitochondrial ATP synthesis and glycolysis is required to sufficiently reduce intracellular ATP levels in RPE cells under our culture conditions. Therefore, we decided to use OM and 2DG to examine the DSB repair capability after IR in this study.

To investigate whether DSBs induced foci formation, which represents the recruitment of each repair protein at DSB sites, under low ATP conditions, γH2AX, MDC1 and 53BP1 foci were analyzed 30 min after IR. The experimental design is shown in Fig. 1B. As ATM kinase activity is required for IR-induced DSB repair and signaling, including DSB repair [19], H2AX phosphorylation [20] and DSB end resection in HR of G2 phase [21], an ATMi was used as a positive control. In this study, foci formation in G1 and G2 phase cells was examined because G1 phase cells predominantly undergo NHEJ, whereas G2 phase cells undergo both NHEJ and HR after IR

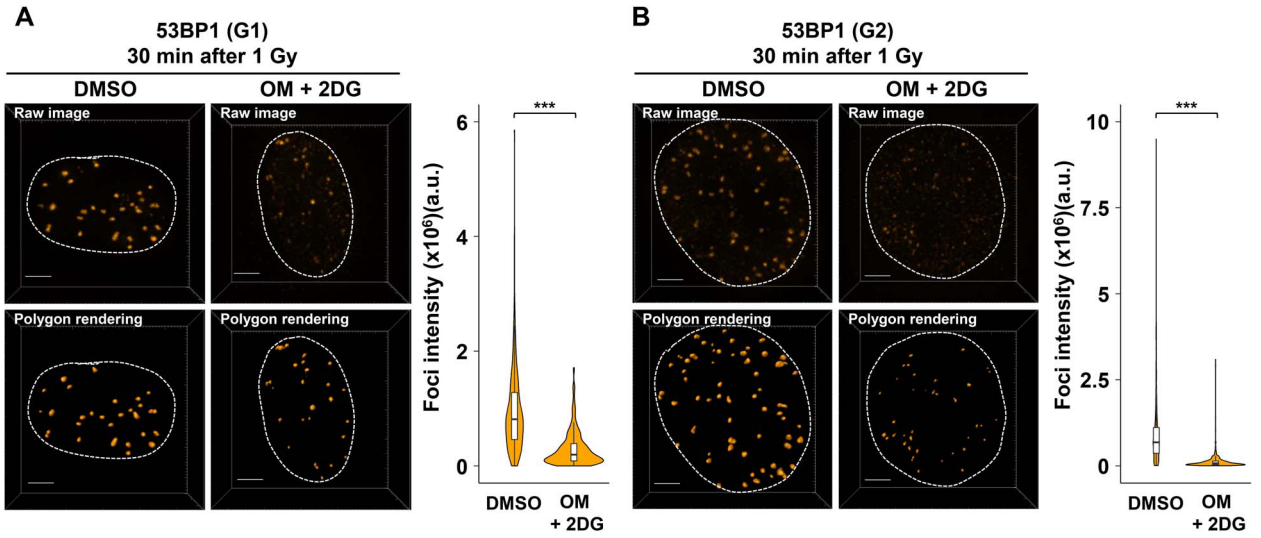

Fig. 3. Analysis of 53BP1 foci intensity under low ATP conditions. RPE cells were irradiated with 1 Gy IR. DMSO or 10 μM OM + 20 mM 2DG were added 2 h before IR irradiation. For G2 phase foci analysis, 3 μM APH was added immediately after IR. (A) The intensity of 53BP1 foci within γH2AX signal in the G1 phase cells was measured by using Imaris 30 min after IR. Quantified result is shown in right panel. (B) The intensity of 53BP1 foci within γH2AX signal in the G2 phase cells was measured by using Imaris 30 min after IR. In both (A) and (B), images were captured using a DeltaVision OMX. Polygon rendering was generated using Imaris as representative images. Quantified result is shown in right panel. Similar results were obtained in two independent experiments. Scale bar, 3 μm. The number of analyzed foci (DMSO: $n = 307$, OM + 2DG: $n = 289$, for G1; DMSO: $n = 564$, OM + 2DG: $n = 623$, for G2).

[21]. We found that the formation of γH2AX and MDC1 foci was not impaired in the presence of OM and 2DG (Fig. 1C and D [γH2AX in G1 and G2, respectively] and Fig. 1E and F [MDC1 in G1 and G2, respectively]). By contrast, the number of 53BP1 foci was modestly but significantly reduced (Fig. 1G [G1] and Fig. 1H [G2]). Representative images of repair foci analyzed under low ATP conditions are shown in Fig. 2A–F. Because a significant reduction in 53BP1 foci number was observed under low ATP conditions, the signal intensity of 53BP1 was measured. We found that the intensity of 53BP1 foci in both G1 and G2 phases under low ATP conditions was smaller than that in DMSO-treated control cells, and some foci signal showed almost background levels (Fig. 3A and B).

To investigate whether the activity of ATM, which is a central kinase in DNA damage response, is affected by ATP shortage, ATM autophosphorylation was examined at 30 min after IR. However, an obvious change was not observed following the treatment with OM + 2DG for 2 h, which is a condition in this study (Supplementary Fig. 1A). We also attempted to examine the DSB repair kinetics under low ATP conditions using an assay for DSB repair kinetics by monitoring γH2AX foci disappearance [20]; however, as long-term culture (8 h post-IR) induced DSBs even without IR (data not shown), the assay was not performed.

Next, to investigate whether low ATP levels influenced HR-associated foci formation, BRCA1, RPA and RAD51 foci were examined in G2 phase cells 2 h after IR (Fig. 1B). We found that BRCA1 and RPA foci formation decreased under low ATP conditions compared with that in DMSO-treated G2 phase cells (Fig. 4A and B). Notably, the number of RAD51 foci was drastically reduced under low ATP conditions (Fig. 4C). Representative images of BRCA1, RPA and RAD51 foci are shown in Fig. 4D–F. Furthermore, we examined the signal intensity of RPA and RAD51 foci under low ATP conditions. Similar to the results of foci number scoring, the intensity of RPA foci was modestly reduced (Fig. 5A) and the intensity of RAD51 foci was drastically reduced under low ATP conditions (Fig. 5B). This result suggests that a certain level of ATP is essential for RAD51 foci formation after IR. To confirm whether the reduced foci number and intensity were a consequence of low protein expression, the expressions of H2AX, MDC1, 53BP1, BRCA1, RPA and RAD51 were examined. However, an obvious change was not observed following treatment with OM + 2DG for 2 h (Supplementary Fig. 1B), suggesting that the reduction in 53BP1, BRCA1, RPA and RAD51 foci formation is dependent on the impaired DNA damage response, rather than protein expression, under the condition of this study.

DISCUSSION

In the present study, we found that 53BP1 foci formation was modestly reduced in both G1 and G2 phases under low ATP conditions, whereas γH2AX and MDC1 foci formation were not obviously impaired. These results suggest that sufficient cellular ATP levels are required for promoting the recruitment and/or maintenance of 53BP1 to DSB sites after IR. ATM autophosphorylation itself was not significantly changed under low ATP conditions; however, ATP shortage might affect a thousand downstream substrates of ATM in a stepwise manner, which results in a defect in 53BP1 foci formation. This may have resulted in different 53BP1 recruitment deficiencies at different regions

Fig. 4. Inhibition of ATP synthesis impairs HR-associated foci formation in G2 phase cells after IR. (A–C) BRCA1 and RPA foci formation were reduced, and RAD51 foci formation was significantly impaired under low ATP conditions. RPE cells were irradiated with 1 Gy IR. Recruitment of HR factors was analyzed 2 h after IR. To prevent the progression of S phase cells into the G2 phase during analysis, 3 μM APH was added immediately after IR. DMSO or 10 μM OM + 20 mM 2DG were added 2 h before IR. ATMi was added 30 min before IR. A boxplot was generated based on the results of a single experiment. Similar results were obtained in two independent experiments. Statistical analyses were performed for a single experiment. $^{***}P < 0.001$. (D–F) Representative images of IR-induced BRCA1, RPA and RAD51 foci in G2 phase RPE cells 2 h after 1 Gy IR. Irradiated RPE cells were fixed and stained with (D) BRCA1 and CENPF (G2 phase markers), (E) RPA and CENPF and (F) RAD51 and CENPF. DNA was stained with DAPI. Scale bar, 10 μm.

of the genome because not all 53BP1 foci disappeared under low ATP conditions. In addition, we found that HR-associated foci formation was impaired under low ATP conditions. We also found that BRCA1 and RPA foci were not effectively formed, and RAD51 foci formation was more drastically impaired under low ATP conditions. These data suggest that the maintenance of ATP levels is critical for the DSB repair response after IR, particularly the downstream steps in HR, such as RAD51 loading. A model for DSB repair status under low ATP conditions is shown in Fig. 6. As a limitation of this study, the impact of DSB repair capability may differ depending on the level of ATP and duration of ATP shortage. In this study, we examined the foci formation of DSB repair proteins at 30 min to 2 h after IR. As OM and 2DG were added 2 h before IR, the maximal duration of OM and 2DG treatment is 4 h, i.e. the duration of ATP shortage is <4 h. Although we did not observe a substantial reduction in ATM autophosphorylation, i.e. ATM kinase activity itself was normal under this condition, and expression of the repair proteins in this study, different results can be obtained if other conditions were applied.

ATP is involved in several steps in DSB repair, such as DNA ligation, chromatin remodeling and DNA damage signaling via protein kinase and ATPase activities. In addition, DNA nucleases and DNA helicases, which are critical enzymes promoting DSB repair, require ATP. Our study did not clarify the factors that were most influenced; however, as resection and RAD51 loading in G2 phase cells were significantly affected by ATP shortage, we predicted that the reactions involving DNA nucleases and DNA helicases during resection in HR may be inactivated under low ATP conditions. Furthermore, regarding chromatin remodeling, the activity of remodeling factors involved in DSB repair, such as SMARCAD1, INO80, CHD4 and p400, may be comprehensively downregulated under low ATP conditions [22–27]. An interesting question is why RAD51 foci formation was strongly impaired by ATP shortage. Previous studies have shown that ATP promotes the binding of RAD51 to DNA [28, 29]. By contrast, although RAD51 has ATPase activity, its ATP hydrolysis is dispensable for foci formation and DSB repair after IR [30]. As an alternative idea, since RAD51 loading likely requires multiple chromatin remodeling steps, which probably requires a substantial amount of ATP, and an insufficient amount of ATP might cause the failure of RAD51 loading on the single strand region. The identification of the central factor impairing HR activity will be addressed in future studies.

Fig. 5. Analysis of RPA and RAD51 foci intensity under low ATP conditions. RPE cells were irradiated with 1 Gy IR. DMSO or 10 μM OM + 20 mM 2DG were added 2 h before IR irradiation. For G2 phase foci analysis, 3 μM APH was added immediately after IR. (A) The intensity of RPA foci within γH2AX signal in the G2 phase cells was measured 2 h after IR. Quantified result is shown in right panel. (B) The intensity of RAD51 foci within γH2AX signal in the G2 phase cells was measured 30 min after IR. In both (A) and (B), images were captured using a DeltaVision OMX. Polygon rendering was generated using Imaris as representative images. Quantified result is shown in right panel. Similar results were obtained in two independent experiments. Scale bar, 3 μm. The number of analyzed foci (DMSO: *n* = 374, OM + 2DG: *n* = 441, for RPA) (DMSO: *n* = 400, OM + 2DG: *n* = 387, for RAD51).

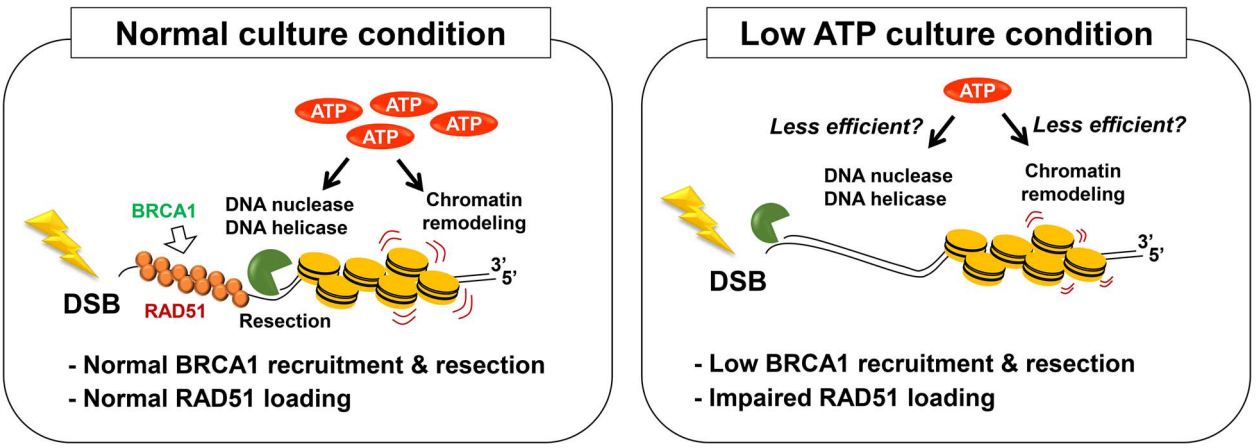

Fig. 6. A model for DSB repair status under low ATP condition. ATP is involved in several steps in DSB repair, such as DNA ligation, chromatin remodeling and DNA damage signaling via protein kinase and ATPase activities. In addition, DNA nucleases and DNA helicases, which are critical enzymes promoting DSB repair, require ATP. This study showed that short-term ATP shortage reduces DSB end resection and almost completely impaired RAD51 recruitment in G2 cells after IR. The impairment of RAD51 loading may be dependent on the lack of multiple pathways in HR process such as DNA nuclease- and DNA helicase-dependent DSB end processing and chromatin remodeling.

CONCLUSIONS

In this study, we found a modest failure of 53BP1 recruitment at DSB sites in both G1 and G2 phase cells, whereas DSB end resection and RAD51 loading were significantly impaired in G2 phase cells under low ATP conditions. Our findings suggest that short-term ATP shortages in the human body, such as cerebral ischemia or myocardial infarction, may influence the quality and pathways of DSB repair after IR. Although cells in cerebral ischemia or myocardial infarction are arrested in the G0/G1 phase that does not utilize the HR pathway [21, 31], resection-mediated NHEJ, which is used in G0/G1

phase, may be affected by the ATP shortage [32, 33]. Further studies are required to elucidate the relationship between the cellular ATP levels and DSB repair in the context of pathological conditions and radiation biology.

SUPPLEMENTARY DATA

Supplementary data are available at *Journal of Radiation Research* online.

ACKNOWLEDGEMENTS

We would like to acknowledge Miki Takahashi and Hiroko Iino for valuable assistance in conducting the laboratory work.

CONFLICT OF INTEREST STATEMENT

The authors declare no conflicts of interest.

FUNDING

This work was supported by JSPS KAKENHI (JP21H03596; AMED under Grant Numbers JP22zf0127008 and JP23zf0127008), Takeda Science Foundation, Sumitomo Foundation, Suntory Foundation for Life Sciences Bioorganic Research Institute, Kobayashi Foundation for Cancer Research, Foundation for Promotion of Cancer Research, Naito Foundation, Princess Takamatsu Cancer Research Fund, Astellas Foundation for Research on Metabolic Disorders, Bristol-Myers Squibb Fund, and National Cancer Center Research and Development Fund (2021-A-8 and 2022-A-8). A part of this study was conducted through the Joint Usage/Research Center Program of the Radiation Biology Center at Kyoto University.

AUTHORS' CONTRIBUTIONS

A.S. (Conceptualization, Methodology, Validation, Writing—Original Draft Preparation, Supervision, Project Administration, Funding Acquisition), Y.U. (Methodology, Validation, Investigation, Writing—Review and Editing), R.H. (Investigation, Writing-Original Draft Preparation), H.O. (Investigation, Writing—Review and Editing), M.I. (Investigation, Writing—Review and Editing), Mo. Y. (Writing—Review and Editing), D.U. (Writing—Review and Editing), R.T.L. (Writing—Review and Editing), Ma. Y. (Writing—Review and Editing), Y.K. (Writing—Review and Editing).

PRESENTATION AT A CONFERENCE

Several parts of this study have been presented at the 66th Annual Meeting of the Japanese Radiation Research Society (JRRS66).

REFERENCES

1. Shibata A, Jeggo PA. DNA double-strand break repair in a cellular context. *Clin Oncol (R Coll Radiol)* 2014;26:243–9. https://doi.org/10.1016/j.clon.2014.02.004.
2. Jackson SP, Bartek J. The DNA-damage response in human biology and disease. *Nature* 2009;461:1071–8. https://doi.org/10.1038/nature08467.
3. Lobrich M, Rief N, Kuhne M. *et al.* In vivo formation and repair of DNA double-strand breaks after computed tomography examinations. *Proc Natl Acad Sci USA* 2005;102:8984–9. https://doi.org/10.1073/pnas.0501895102.
4. Schaue D, McBride WH. Opportunities and challenges of radiotherapy for treating cancer. *Nat Rev Clin Oncol* 2015;12:527–40. https://doi.org/10.1038/nrclinonc.2015.120.
5. Stiff T, O'Driscoll M, Rief N. *et al.* ATM and DNA-PK function redundantly to phosphorylate H2AX after exposure to ionizing radiation. *Cancer Res* 2004;64:2390–6. https://doi.org/10.1158/0008-5472.CAN-03-3207.
6. Shibata A, Barton O, Noon AT. *et al.* Role of ATM and the damage response mediator proteins 53BP1 and MDC1 in the maintenance of G(2)/M checkpoint arrest. *Mol Cell Biol* 2010;30:3371–83. https://doi.org/10.1128/MCB.01644-09.
7. Lu J, Matunis MJ. A mediator methylation mystery: JMJD1C demethylates MDC1 to regulate DNA repair. *Nat Struct Mol Biol* 2013;20:1346–8. https://doi.org/10.1038/nsmb.2729.
8. Lilley CE, Chaurushiya MS, Boutell C. *et al.* A viral E3 ligase targets RNF8 and RNF168 to control histone ubiquitination and DNA damage responses. *EMBO J* 2010;29:943–55. https://doi.org/10.1038/emboj.2009.400.
9. Shi W, Ma Z, Willers H. *et al.* Disassembly of MDC1 foci is controlled by ubiquitin-proteasome-dependent degradation. *J Biol Chem* 2008;283:31608–16. https://doi.org/10.1074/jbc.M801082200.
10. Shibata A, Jeggo PA. Roles for 53BP1 in the repair of radiation-induced DNA double strand breaks. *DNA Repair (Amst)* 2020;93:102915. https://doi.org/10.1016/j.dnarep.2020.102915.
11. Shibata A. Regulation of repair pathway choice at two-ended DNA double-strand breaks. *Mutat Res* 2017;803-805:51–5. https://doi.org/10.1016/j.mrfmmm.2017.07.011.
12. Rothkamm K, Kruger I, Thompson LH. *et al.* Pathways of DNA double-strand break repair during the mammalian cell cycle. *Mol Cell Biol* 2003;23:5706–15. https://doi.org/10.1128/MCB.23.16.5706-5715.2003.
13. Sartori AA, Lukas C, Coates J. *et al.* Human CtIP promotes DNA end resection. *Nature* 2007;450:509–14. https://doi.org/10.1038/nature06337.
14. Gravel S, Chapman JR, Magill C, Jackson SP. DNA helicases Sgs1 and BLM promote DNA double-strand break resection. *Genes Dev* 2008;22:2767–72. https://doi.org/10.1101/gad.503108.
15. Nimonkar AV, Genschel J, Kinoshita E. *et al.* BLM-DNA2-RPA-MRN and EXO1-BLM-RPA-MRN constitute two DNA end resection machineries for human DNA break repair. *Genes Dev* 2011;25:350–62. https://doi.org/10.1101/gad.2003811.
16. Daley JM, Jimenez-Sainz J, Wang W. *et al.* Enhancement of BLM-DNA2-mediated long-range DNA end resection by CtIP. *Cell Rep* 2017;21:324–32. https://doi.org/10.1016/j.celrep.2017.09.048.
17. Isono M, Niimi A, Oike T. *et al.* BRCA1 directs the repair pathway to homologous recombination by promoting 53BP1

dephosphorylation. *Cell Rep* 2017;18:520–32. https://doi.org/10.1016/j.celrep.2016.12.042.
18. Sifat AE, Nozohouri S, Archie SR. *et al.* Brain energy metabolism in ischemic stroke: effects of smoking and diabetes. *Int J Mol Sci* 2022;23:8512. https://doi.org/10.3390/ijms23158512.
19. Goodarzi AA, Noon AT, Deckbar D. *et al.* ATM signaling facilitates repair of DNA double-strand breaks associated with heterochromatin. *Mol Cell* 2008;31:167–77. https://doi.org/10.1016/j.molcel.2008.05.017.
20. Lobrich M, Shibata A, Beucher A. *et al.* gammaH2AX foci analysis for monitoring DNA double-strand break repair: strengths, limitations and optimization. *Cell Cycle* 2010;9:662–9. https://doi.org/10.4161/cc.9.4.10764.
21. Shibata A, Conrad S, Birraux J. *et al.* Factors determining DNA double-strand break repair pathway choice in G2 phase. *EMBO J* 2011;30:1079–92. https://doi.org/10.1038/emboj.2011.27.
22. Chakraborty S, Pandita RK, Hambarde S. *et al.* SMARCAD1 phosphorylation and ubiquitination are required for resection during DNA double-strand break repair. *iScience* 2018;2:123–35. https://doi.org/10.1016/j.isci.2018.03.016.
23. Gospodinov A, Vaissiere T, Krastev DB. *et al.* Mammalian Ino80 mediates double-strand break repair through its role in DNA end strand resection. *Mol Cell Biol* 2011;31:4735–45. https://doi.org/10.1128/MCB.06182-11.
24. van Attikum H, Gasser SM. Crosstalk between histone modifications during the DNA damage response. *Trends Cell Biol* 2009;19:207–17. https://doi.org/10.1016/j.tcb.2009.03.001.
25. Luijsterburg MS, Acs K, Ackermann L. *et al.* A new non-catalytic role for ubiquitin ligase RNF8 in unfolding higher-order chromatin structure. *EMBO J* 2012;31:2511–27. https://doi.org/10.1038/emboj.2012.104.
26. Pan MR, Hsieh HJ, Dai H. *et al.* Chromodomain helicase DNA-binding protein 4 (CHD4) regulates homologous recombination DNA repair, and its deficiency sensitizes cells to poly(ADP-ribose) polymerase (PARP) inhibitor treatment. *J Biol Chem* 2012;287:6764–72. https://doi.org/10.1074/jbc.M111.&break;287037.
27. Courilleau C, Chailleux C, Jauneau A. *et al.* The chromatin remodeler p400 ATPase facilitates Rad51-mediated repair of DNA double-strand breaks. *J Cell Biol* 2012;199:1067–81. https://doi.org/10.1083/jcb.201205059.
28. Baumann P, Benson FE, West SC. Human Rad51 protein promotes ATP-dependent homologous pairing and strand transfer reactions in vitro. *Cell* 1996;87:757–66. https://doi.org/10.1016/S0092-8674(00)81394-X.
29. Sung P, Robberson DL. DNA strand exchange mediated by a RAD51-ssDNA nucleoprotein filament with polarity opposite to that of RecA. *Cell* 1995;82:453–61. https://doi.org/10.1016/0092-8674(95)90434-4.
30. Morrison C, Shinohara A, Sonoda E. *et al.* The essential functions of human Rad51 are independent of ATP hydrolysis. *Mol Cell Biol* 1999;19:6891–7. https://doi.org/10.1128/MCB.19.10.6891.
31. Beucher A, Birraux J, Tchouandong L. *et al.* ATM and Artemis promote homologous recombination of radiation-induced DNA double-strand breaks in G2. *EMBO J* 2009;28:3413–27. https://doi.org/10.1038/emboj.2009.276.
32. Biehs R, Steinlage M, Barton O. *et al.* DNA double-strand break resection occurs during non-homologous end joining in G1 but is distinct from resection during homologous recombination. *Mol Cell* 2017;65:671–684.e5. https://doi.org/10.1016/j.molcel.2016.12.016.
33. Yasuhara T, Kato R, Yamauchi M. *et al.* RAP80 suppresses the vulnerability of R-loops during DNA double-strand break repair. *Cell Rep* 2022;38:110335. https://doi.org/10.1016/j.celrep.2022.110335.